Diffraction of short waves modelled using new mapped wave envelope finite and infinite elements

Edmund Chadwick
Peter Bettess
and Omar Laghrouche
School of Engineering, University of Durham,
Science Laboratories, South Road
Durham DH1 3LE, England

June 2, 1997

SUMMARY

We consider a two dimensional wave diffraction problem from a closed body such that the complex progressive wave potential satisfies the Sommerfield condition and the Helmholtz equation. We are interested in the case where the wavelength is much smaller than any other length dimensions of the problem. We introduce new mapped wave envelope infinite elements to model the potential in the far field, and test them for some simple Dirichlet boundary condition problems. They are used in conjuction with wave envelope finite elements developed earlier [1] to model the potential in the near field. An iterative procedure is used in which an initial estimate of the phase is iteratively improved. The iteration scheme, by which the wave envelope and phase are recovered, is described in detail.

KEY WORDS : Wave diffraction, finite elements, infinite elements, wave enevelope, iterated phase.

1 Introduction

Short wave diffraction problems are those in which the wavelength is much smaller than any of the dimensions of the problem. Such problems arise in surface waves on water, acoustics and pressure waves, electromagnetic waves and elastic waves. They are of considerable economic importance, but the general problem is still not solved. For exterior wave problems, there is a difficulty in modelling the far field potential. This is because ten nodes per wavelength are needed to model the oscillatory variation of the potential which remains present in the far field. Thus it has been necessary to develop large elements which cover many wavelengths, and also infinite elements.

The first idea for this development was by Bettess and Zienkiewicz [2], [3] and incorporated the harmonic variation of the potential into the shape function. Mapped infinite elements for wave envelope decay $r^{-1/2}$ of the diffraction potential was then given in another paper [4]. The determination of the resulting integral expression proved complicated, and special integration rules were developed. Astley [5], [6], [7] later introduced a *complex conjugate* weighting, which simplifies the integrand greatly so that it can be evaluated using Gauss-Legendre integration. Chadwick and Bettess [1], [8] give an equivalent approach for bounded finite domain problems by choosing the governing equation for the wave envelope and the phase rather than for the potential. An iterative method is developed for two dimensional problems whereby an estimate of the phase is first given, from the finite element calculation for the wave envelope, a better estimate for the phase is obtained. The standard Galerkin shape and weighting functions can then be used.

In the present paper this approach is extended for exterior problems. The motivation is to develop a general method for short wave diffraction problems, in which the discretization is almost independent of the wavelength. We start with the differential equation for the wave envelope A and phase p rather than the Helmholtz equation for the potential ϕ, where $\phi = Ae^{ip}$. We introduce new mapped wave envelope infinite elements to model the potential in this domain. The first formulation we introduce uses the usual infinite element mapping functions [9] and shape functions [4], without the oscillation term e^{ip}, for the wave envelope. The weighting functions are chosen to be the same as the shape functions. The second formulation is obtained by applying the divergence theorem to the governing integral matrix, resulting in a Hermitian matrix added to a contour integral enclosing the domain at infinity. The contour integral gives a finite contribution which is calculated in terms of the angles by which the finite element is subtended. If different weighting functions, multiplied by an additional factor r^{-1}, are considered then a third formulation is obtained in which the contour integral contribution is zero. This gives an Astley-type [7] mapped wave envelope formulation. The three formulations are tested for some simple problems. A diffraction problem, from a cylinder of radius a, is then considered. The robustness of the iteration method is investigated using the Hankel source potential and the wave diffraction potential past a cylinder by considering the convergence for different phase estimates and different values of the wavenumber k.

2 The model equations

In this section we derive the governing differential equation for the wave envelope and the phase from the time dependent wave equation. This is given by [10] :

$$\frac{\partial^2 \Phi}{\partial t^2} = c^2 \nabla^2 \Phi \tag{1}$$

for the time dependent wave potential $\Phi(x, y, t)$ where x and y are the two-dimensional cartesian coordinates, t is time, c is a constant defined as the wave speed and ∇^2 is the Laplacian operator. We assume the time variation is such that $\Phi = \phi e^{-i\omega t}$ where ϕ is a function of x and y and ω is the circular frequency. Hence the time independent wave potential ϕ is given by the Helmholtz equation :

$$(\nabla^2 + k^2)\phi = 0 \tag{2}$$

where $k = \omega/c$ is the wavenumber. We look for progressive wave solutions of the form :

$$\phi = Ae^{ip} = Ae^{iks} \tag{3}$$

where A is the wave envelope and p is the phase. A and p are real. Hence s is defined as $s = p/k$. Substituting (3) into (2) gives the governing differential equation :

$$k^2 A \left(1 - \underline{\nabla s}.\underline{\nabla s}\right) + ik\left(2\underline{\nabla A}.\underline{\nabla s} + A\nabla^2 s\right) + \nabla^2 A = 0 \tag{4}$$

where $\underline{\nabla}$ is the gradient vector operator. In order to construct the governing integrals used in the finite element formulation we consider the integral :

$$\int\int_\Omega f\left[k^2 A \left(1 - \underline{\nabla s}.\underline{\nabla s}\right) + ik\left(2\underline{\nabla A}.\underline{\nabla s} + A\nabla^2 s\right) + \nabla^2 A\right] dxdy = 0 \tag{5}$$

for some continuous weighting function $f(x, y)$ defined over the space $[\Omega]$, where the area Ω is bounded by a closed contour over a body Γ_B and a circle circumference contour Γ_R of radius R (figure 1). The integral is assumed to be determinate. Assuming $\underline{\nabla f}$ is also defined over the area Ω then using the divergence theorem, expression (5) can be expressed as :

$$\int\int_{\Omega}\left[-\underline{\nabla f}.\underline{\nabla A}+k^2 fA\left(1-\underline{\nabla s}.\underline{\nabla s}\right)+ikf\left(2\underline{\nabla A}.\underline{\nabla s}+A\nabla^2 s\right)\right]dxdy \\ +\int_{\Gamma_R} f\underline{\nabla A}.\underline{n}d\Gamma-\int_{\Gamma_B} f\underline{\nabla A}.\underline{n}d\Gamma=0 \quad (6)$$

where $\underline{n}$ is the outward pointing normal to the inner domain closed by the contour Γ_B.

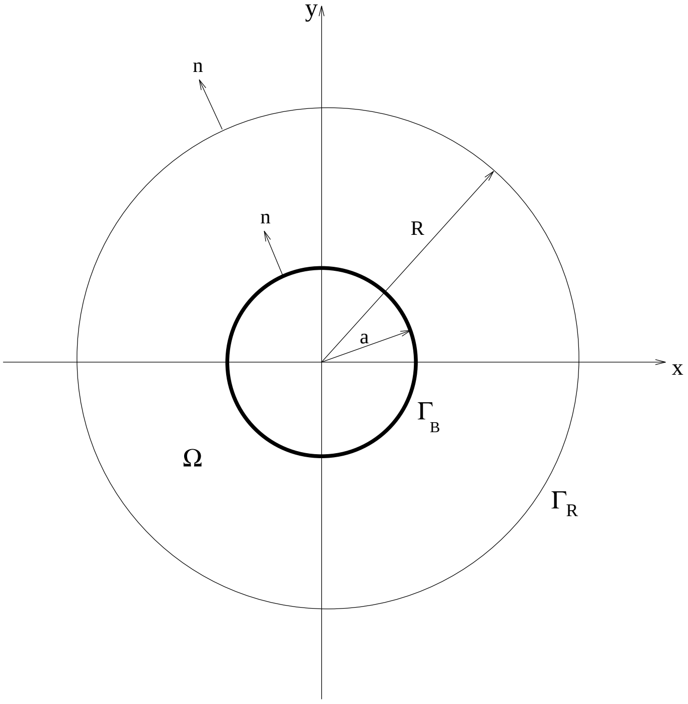

Figure 1: Wave diffraction by a cylinder - schematic diagram of the studied problem.

To solve the system (6), the inner field $a \leq r \leq R$ is treated using finite elements and the far field $r > R$ is analyzed using infinite elements. Since finite elements are described in many finite elements references, only infinite elements will be developed in this paper.

3 Formulation of a 2-D wave envelope infinite element

In this section we give a mapping of the infinite domain far field elements explicitly, from which the mapping functions [9] are obtained exactly. We then give the approximate mapping for the polar angle θ variation when the angle subtended by the infinite element is small.

Consider the six node infinite element of figure 2 with nodes at positions (r_0, θ_1), $(2r_0, \theta_1)$, (r_0, θ_2), $(2r_0, \theta_2)$, (r_0, θ_3) and $(2r_0, \theta_3)$ respectively in cylindrical polar coordinates. This implies that the infinite elements are exterior to a circular boundary. This is a restriction, which it should be possible to remove, but for the present is a useful simplification. Thus the infinite element region is $r \geq r_0$, $\theta_1 \leq \theta \leq \theta_3$. The multivalued function θ (we may add or subtract $2\pi n$, where n is an integer) is chosen to vary continuously across the infinite element. We consider new variables (ξ, η) such that the infinite element domain is mapped into the finite space $-1 \leq \xi \leq 1$, $-1 \leq \eta \leq 1$ (figure 2).

Let us consider the mapping given by :

$$r = \frac{2r_0}{1-\xi} \tag{7}$$

and :

$$e^{i\theta} = e^{i\theta_1}\left[-(1/2)\eta(1-\eta)\right] + e^{i\theta_2}\left[(1+\eta)(1-\eta)\right] + e^{i\theta_3}\left[(1/2)\eta(1+\eta)\right] \tag{8}$$

If the angle subtended by the element is small, then to first order using the Taylor series expansion, expression (8) becomes :

$$\theta = \theta_1\left[-(1/2)\eta(1-\eta)\right] + \theta_2\left[(1+\eta)(1-\eta)\right] + \theta_3\left[(1/2)\eta(1+\eta)\right] \tag{9}$$

This is equivalent to approximating the circle circumference arc boundary of the infinite element with a quadratic variation in θ. Thus as the angle subtended becomes small, we obtain a better approximation.

The usual mapping functions [9] are given exactly from (7) and (9) since :

$$x = r\cos\theta = \sum_{j=1}^{6} M_j x_j$$
$$y = r\sin\theta = \sum_{j=1}^{6} M_j y_j \tag{10}$$

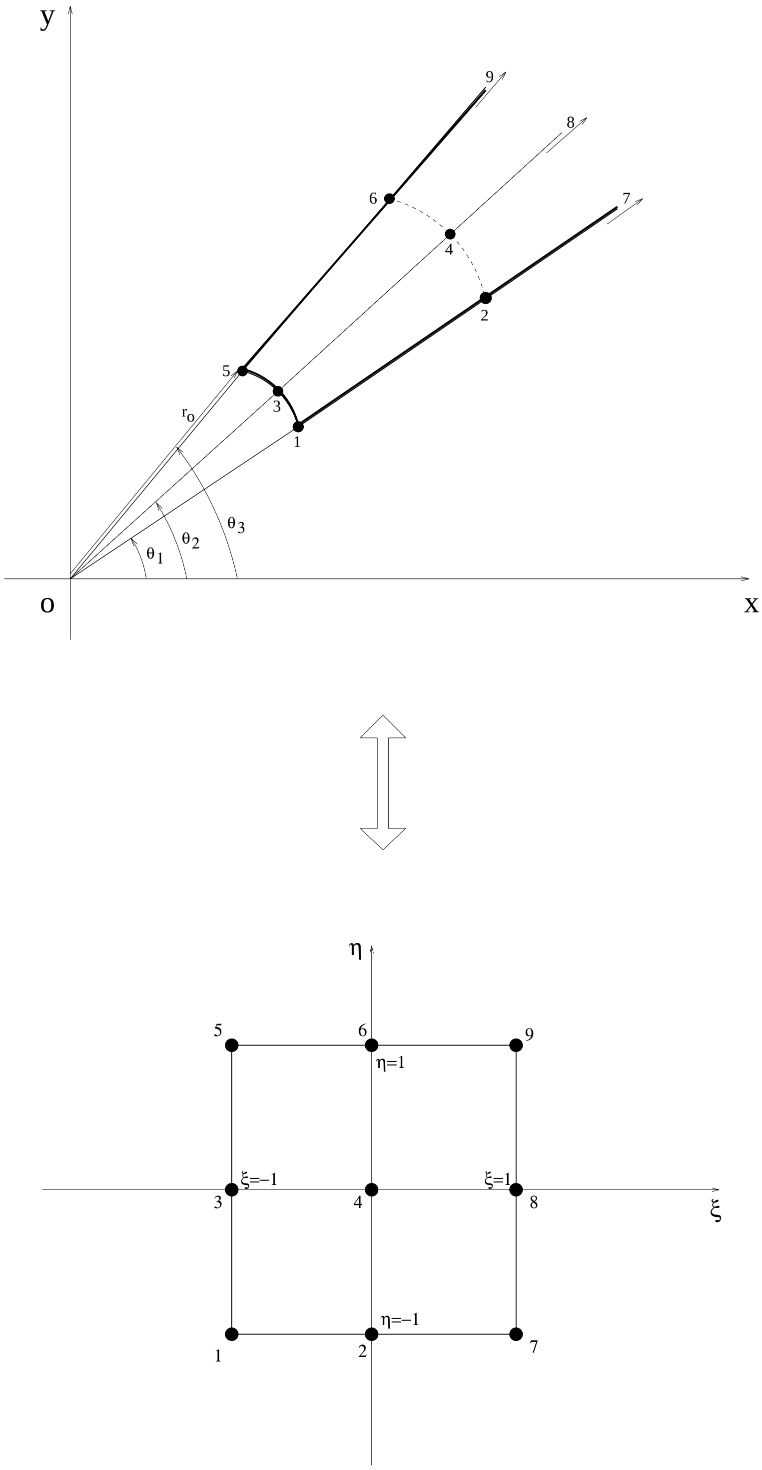

Figure 2: Two dimensional mapped infinite element.

where x_i and y_i are the cartesian coordinates of node j and M_j is the mapping function for node j :

$$
\begin{aligned}
M_1 &= \left(-\frac{2\xi}{1-\xi}\right)[-(1/2)\eta(1-\eta)] \\
M_2 &= \left(\frac{1+\xi}{1-\xi}\right)[-(1/2)\eta(1-\eta)] \\
M_3 &= \left(-\frac{2\xi}{1-\xi}\right)[(1+\eta)(1-\eta)] \\
M_4 &= \left(\frac{1+\xi}{1-\xi}\right)[(1+\eta)(1-\eta)] \\
M_5 &= \left(-\frac{2\xi}{1-\xi}\right)[(1/2)\eta(1+\eta)] \\
M_6 &= \left(\frac{1+\xi}{1-\xi}\right)[(1/2)\eta(1+\eta)]
\end{aligned}
\tag{11}
$$

We assume, in the far field, the wave envelope varies as :

$$A(r,\theta) = \frac{\alpha(\theta)}{\sqrt{r}} + \frac{\beta(\theta)}{r\sqrt{r}} + O(\frac{1}{r^2\sqrt{r}}) \tag{12}$$

and the phase varies as :

$$s(r,\theta) = r + \gamma(\theta) + O(\frac{1}{r}) \tag{13}$$

where $\alpha(\theta)$, $\beta(\theta)$ and $\gamma(\theta)$ are some well behaved continuous functions of θ. We note that a far field potential of this form satisfies the Sommerfeld radiation condition [11] given in two dimensions by Rellich [12] :

$$\lim_{r\to\infty} \sqrt{r}\left(\frac{\partial\phi}{\partial r} - ik\phi\right) = 0 \tag{14}$$

and is to first order given by the potential :

$$\phi(r,\theta) = \frac{\alpha(\theta)}{\sqrt{r}} e^{ikr} \tag{15}$$

The expression of ϕ given in (15) is the first order term in the asymptotic expansion for large kr for any of the Hankel functions of the first kind of integer order [13].

In this formulation we model the wave envelope from the differential equation for the wave envelope rather than for the potential. Hence we use the usual shape function variation [4] but without the oscillation term e^{ikr}. Assuming a Lagrangian quadratic variation in the θ variable given by (9), then from (7) and (12) the variation in A to order $\frac{1}{r^2\sqrt{r}}$ is given by :

$$A = \sum_{j=1}^{6} N_j A_j \tag{16}$$

where A_j is the wave envelope and N_j is the shape function at node j. The shape functions are expressed by :

$$\begin{aligned}
N_1 &= \left[-\frac{\xi}{\sqrt{2}}\sqrt{1-\xi}\right][-(1/2)\eta(1-\eta)] \\
N_2 &= \left[(1+\xi)\sqrt{1-\xi}\right][-(1/2)\eta(1-\eta)] \\
N_3 &= \left[-\frac{\xi}{\sqrt{2}}\sqrt{1-\xi}\right][(1+\eta)(1-\eta)] \\
N_4 &= \left[(1+\xi)\sqrt{1-\xi}\right][(1+\eta)(1-\eta)] \\
N_5 &= \left[-\frac{\xi}{\sqrt{2}}\sqrt{1-\xi}\right][(1/2)\eta(1+\eta)] \\
N_6 &= \left[(1+\xi)\sqrt{1-\xi}\right][(1/2)\eta(1+\eta)]
\end{aligned} \tag{17}$$

The variation of the phase is modelled by :

$$s = \sum_{j=1}^{6} M_j s_j \tag{18}$$

where s_j is the phase at node j. The shape functions are the same as the mapping functions of expression (11).

4 Application : Dirichlet boundary condition problem

Assuming the variation of the wave envelope A and the phase s as given by (12) and (13), and that the weighting function f in expression (6) is of order $A(r,\theta)$, then the contour integral over Γ_R :

$$\int_{\Gamma_R} f\underline{\nabla A}.\underline{n}d\Gamma = O\left(\frac{1}{\sqrt{R}}.\frac{1}{R\sqrt{R}}.R\right) = O\left(\frac{1}{R}\right) \tag{19}$$

tends to zero as R tends to infinity. We consider weighting functions at the unconstrained nodes and shall therefore consider the function $f(x,y)$ equal to zero along the boundary Γ_B. The integral (6) then becomes :

$$\int\int_{\Omega} \left[-\underline{\nabla f}.\underline{\nabla A} + k^2 f A \left(1 - \underline{\nabla s}.\underline{\nabla s}\right) + ikf\left(2\underline{\nabla A}.\underline{\nabla s} + A\nabla^2 s\right)\right] dxdy = 0 \tag{20}$$

The Dirichlet boundary condition is specified on the body contour Γ_B, so ϕ needs to be determined within the domain only. Using expression (20), three formulations are considered :

4.1 First formulation

We consider shape functions N_j which assume $\frac{1}{\sqrt{r}}$ decay for the far field wave envelope, and weighting functions W_l which are the same as the shape functions. Hence expression (20) becomes :

$$\sum_{j=1}^{n} \int\int_{\Omega} [k^2 W_l N_j (1 - \underline{\nabla s}.\underline{\nabla s}) + ikW_l(2\underline{\nabla N_j}.\underline{\nabla s} + N_j \nabla^2 s) - \underline{\nabla W_l}.\underline{\nabla N_j}] dxdy A_j = 0_l \tag{21}$$

where j is summed over all nodes including boundary nodes. Hence the boundary condition gives A_j at constrained nodes, and j is given at all unconstrained nodes.

4.2 Second formulation

Applying the divergence theorem to (21) gives :

$$\sum_{j=1}^{n} \{\int\int_{\Omega} [k^2 W_l N_j (1 - \underline{\nabla s}.\underline{\nabla s}) + ik(W_l \underline{\nabla N_j}.\underline{\nabla s} - N_j \underline{\nabla W_l}.\underline{\nabla s}) \\ - \underline{\nabla W_l}.\underline{\nabla N_j}] dxdy + ik \int_{\Gamma_R} W_l N_j \underline{\nabla s}.\underline{n} d\Gamma\} A_j = 0_l \tag{22}$$

which is similar to the formulation given by Astley for far field wave envelope elements if we assume $\underline{\nabla s}$ is equal to the unit normal in the radial direction. We note however that the first formulation does not include a contour integral at infinity. This contour integral can either be evaluated over each element, or can be eliminated by considering different weighting functions. First, we consider evaluating it. This contribution is finite and can be evaluated for each infinite element by assuming that the variation in θ is given by (9). Since we assume both that the phase is varying as r (13) and $\theta_3 - \theta_1$ is small, then using the expression (9) the contour integral of expression (22) becomes:

$$C = 2ikr_0 \int_{-1}^{1} F_j(\xi,\eta) F_l(\xi,\eta) \frac{d\theta}{d\eta} d\eta \tag{23}$$

where :

$$\begin{aligned}
F_1 &= \frac{1}{2\sqrt{2}}\eta(1-\eta) \\
F_2 &= -\eta(1-\eta) \\
F_3 &= -\frac{1}{\sqrt{2}}(1-\eta)(1+\eta) \\
F_4 &= 2(1-\eta)(1+\eta) \\
F_5 &= -\frac{1}{2\sqrt{2}}\eta(1+\eta) \\
F_6 &= \eta(1+\eta)
\end{aligned} \tag{24}$$

and :

$$\frac{d\theta}{d\eta} = \theta_1(-1/2+\eta) + \theta_2(-\eta) + \theta_3(1/2+\eta) \tag{25}$$

Thus the integral contributions can be determined explicitly, and are given in the appendix. In particular, we give the evaluations obtained using maple. Alternatively, we may eliminate the contour integral by considering a third formulation with different weighting functions.

4.3 Third formulation

We consider Astley's approach [7] using weighting functions of lower order in the field variable r so that the contour integral contribution tends to zero as r tends to infinity. The natural choice would be to obtain the weighting functions by multiplying the shape functions by a factor $\frac{\alpha}{\sqrt{r}}$ where α is chosen so that the function has nodal value one. Hence in the mapped domain (ξ,η) the weighting functions are polynomials quadratic in ξ and η. However, this leads to element matrix integrals in the ξ-plane of the type $\int_{-1}^{1}\sqrt{1-\xi}d\xi$ and $\int_{-1}^{1}\xi\sqrt{1-\xi}d\xi$ to first order. Evaluating these integrals using 2-point Gauss-Legendre numerical integration gives an error of 1% and 8% respectively. Thus these integrals need to be approximated by higher order polynomials, and so higher point Gauss Legendre integration formula need to be considered. Alternatively, we multiply the weighting functions by $\frac{\beta}{r}$, where β is chosen so that the weighting functions have nodal value one. This leads to integrals quadratic in ξ. Hence in the (ξ, η) mapped space, the weighting functions are given by :

$$\begin{aligned}
W_1 &= \left(\frac{\sqrt{1-\xi}}{\sqrt{2}}\right)[(-1/2)\xi(1-\xi)]\,[-(1/2)\eta(1-\eta)] \\
W_2 &= \left(\sqrt{1-\xi}\right)[(1+\xi)(1-\xi)]\,[-(1/2)\eta(1-\eta)] \\
W_3 &= \left(\frac{\sqrt{1-\xi}}{\sqrt{2}}\right)[(-1/2)\xi(1-\xi)]\,[(1+\eta)(1-\eta)] \\
W_4 &= \left(\sqrt{1-\xi}\right)[(1+\xi)(1-\xi)]\,[(1+\eta)(1-\eta)] \\
W_5 &= \left(\frac{\sqrt{1-\xi}}{\sqrt{2}}\right)[(-1/2)\xi(1-\xi)]\,[(1/2)\eta(1+\eta)] \\
W_6 &= \left(\sqrt{1-\xi}\right)[(1+\xi)(1-\xi)]\,[(1/2)\eta(1+\eta)]
\end{aligned} \tag{26}$$

Since the contour integral is zero, the governing integral formulation is given by :

$$\sum_{j=1}^{n} \int\int_{\Omega} [k^2 W_l N_j (1 - \underline{\nabla s}.\underline{\nabla s}) + ik(W_l \underline{\nabla N_j}.\underline{\nabla s} - N_j \underline{\nabla W_l}.\underline{\nabla s})$$
$$-\underline{\nabla W_l}.\underline{\nabla N_j}]dxdyA_j = 0_l \tag{27}$$

In the above formulations, a value for the phase must first be given. An iteration procedure is used whereby, from the initial estimate for the phase, a 'better estimate' is determined from the solution for the wave envelope. This procedure, given next, is described in more detail in [1].

5 A new estimate for the phase function

We consider an iterative method whereby an estimate of the phase $p_0 = ks_0$ is first given and from the resulting finite element calculation for the wave enevelope A_0 a better estimate $p = ks_1$ is obtained. Since p_0 is an estimate for the phase p, A_0 is expected to have an imaginary part. We consider the new estimate ks_1 for the phase such that the potential ϕ_0 satisfies :

$$\phi_0 = A_0 e^{iks_0} = |A_0| e^{i(ks_0 + \beta_0)} = |A_0| e^{iks_1} \tag{28}$$

Hence :

$$s_1 = s_0 - \frac{i}{k} \ln \left\{ \frac{A_0}{|A_0|} \right\} \tag{29}$$

The element matrix integral is evaluated by using the Gauss-Legendre approximation [9]. The new estimate for the phase gradient which is $\underline{\nabla s_1}$ can therefore be calculated at the Gaussian points by :

$$\underline{\nabla s_1} = \underline{\nabla s_0} + \frac{1}{k}\underline{\nabla \beta_0} \tag{30}$$

The gradient of s is stored at each iteration and the 'error' added to it after the wave envelope is determined. For formulation 1, the term $\nabla^2 s_1$ must be evaluated at the Gaussian points : $\underline{\nabla s_1}$ is given at the nodes of the element by assuming the variation (18) and $\underline{\nabla^2 s_1}$ is obtained by differentiating through to find the second derivatives with respect to x and y at the Gaussian points.

Hence an iteration procedure occurs and is stopped when the imaginary part of the wave envelope is negligible. Thus it is hoped that the iteration procedure converges to the actual values for the wave envelope and phase function. For the particular test examples considered, this is found to be the case. It is possible that other iterative schemes could be derived for the coupled equation, possibly finding both amplitude and phase simultaneously. These could be based, for example, on the Newton-Raphson method. We have not yet explored this. The three formulations are now tested for some simple problems.

6 Numerical results

We shall first consider the accuracy of the formulations for infinite elements, and then test the iteration method over a mesh with both finite and infinite elements.

For all the numerical results, we shall use two potentials : The first potential is the 2-D wave Hankel source [13] (Hankel function of order zero) :

$$\phi = H_0(kr) \tag{31}$$

The second is the wave diffraction potential past a circular cylinder given by Havelock [14] and also by MacCamy and Fuchs [15] :

$$\phi = -H_0(kr)\frac{J_0'(ka)}{H_0'(ka)} - \sum_{n=1}^{\infty} 2i^n \cos n\theta [J_n(kr) - \frac{J_n'(ka)}{H_n'(ka)}H_n(kr)] \tag{32}$$

where a is the radius of the cylinder. We shall choose a equal to unity. Since both potentials are symmetric about the x-axis, we shall consider the domain

$y > 0$ only. All results will be presented in non dimensionalised form. They are normalised with respect to the cylider radius a.

6.1 Accuracy over infinite elements

We find that the best results are obtained by further constraining the phase in the infinite element region; We make a further approximation in the infinite element domain : We assume that the gradient of the phase $\underline{\nabla s}$ varies as $\hat{r}$, the unit vector in the radial r-direction. The term in the integrand :

$$k^2(1 - \underline{\nabla s}.\underline{\nabla s})$$

is then identically zero. The infinite elements constrained in this way for the third formulation are the Astley wave envelope infinite elements described in [7].

We test the accuracy of the three formulations. First, we compare the three formulations for the Hankel source potential. We shall find that the third formulation is the most accurate. The accuracy of this formulation is further tested with the Havelock diffraction potential. In this subsection, the wave envelope is calulated using the exact values of the phase as an initial guess, so no iteration is needed.

6.1.1 Accuracy of the three formulations

The tests are carried out using the Hankel source as a Dirichlet boundary condition. We consider an infinite element mesh in the region $y > 0$ (figure 3).

The constraints are applied at the nodes along $y = 0$ and $r = 5$. The wave number considered is $k = 2\pi$ which corresponds to a nodal spacing of five wavelengths in the direction of propagation. We give the results for the relative error in the wave envelope at each node in the infinite element region, these being the circumferential nodes situated at $r = 10$.

As shown by figure 4, the relative error does not exceed 1.5 per cent for the three formulations.

Formulation 1 gives the the biggest error. This is probably because a Laplacian in the phase $\nabla^2 s$ is evaluated with this formulation, which entails two Jacobian transformations, rather than one for $\underline{\nabla s}$, and we would therefore expect a greater error in the approximation of $\nabla^2 s$.

In the second formulation, a contour integral at infinity is evaluated using the expressions given in the appendix. Lower order weighting functions are

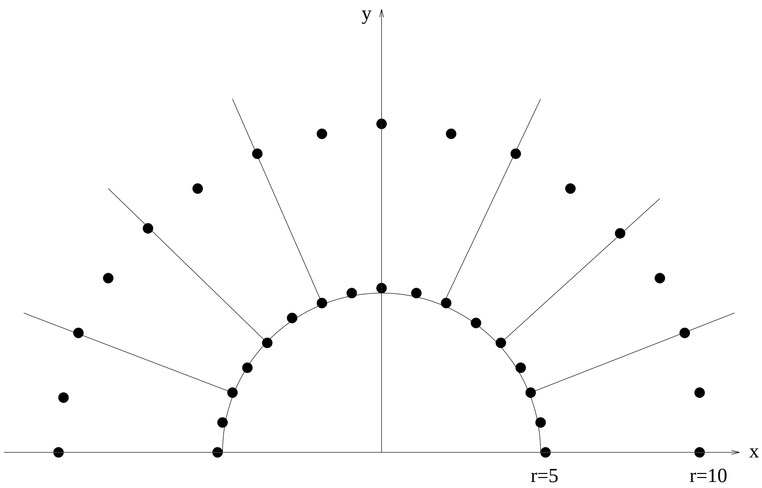

Figure 3: Position of infinite elements.

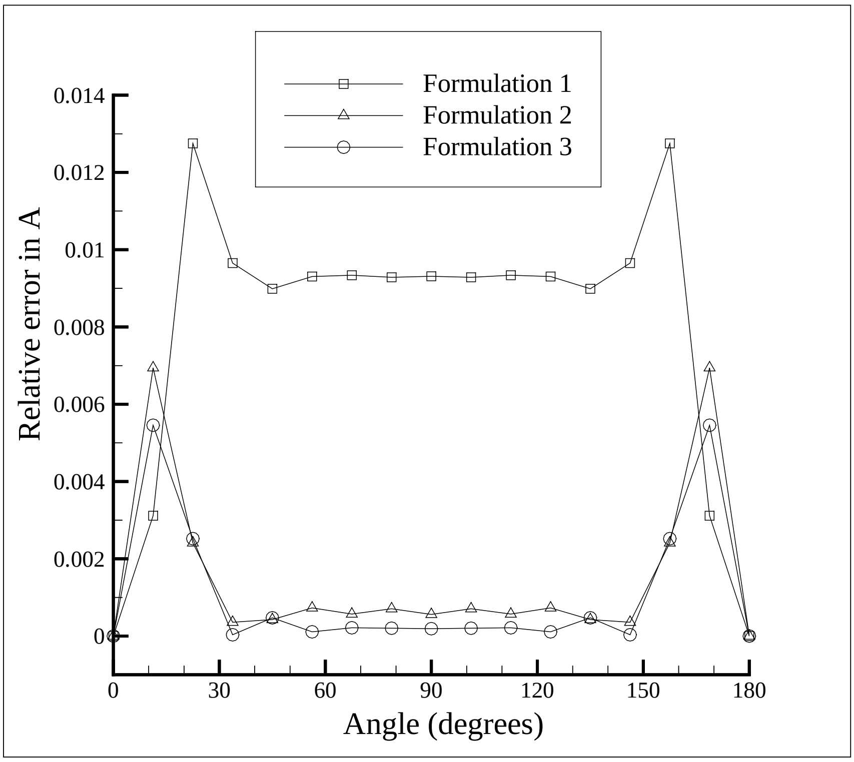

Figure 4: Relative error in wave envelope along $r = 10$.

used in the third formulation to avoid this evaluation, and from figure 4 it is seen that this gives greater accuracy. We therefore shall only use the third formulation, which uses Astley wave envelope infinite elements [7], to model the infinite element domain in the rest of the paper.

6.1.2 Accuracy for a wave diffraction potential

The same problem is considered but this time we apply the Havelock diffraction potential [14] as a Dirichlet boundary condition. The mesh for this problem is similar to the one represented in figure 3, in this case, with infinite elements starting from $r = 6$.

We note that this is an artificial boundary condition since the velocity rather than the potential should be given at nodes on the cylinder boudary $r = 6$. The wave number is taken this time to be equal to $\pi/2$ which corresponds to a nodal spacing of 1.5 wavelengths in the direction of wave propagation. The variation of the wave envelope obtained numerically is presented as well as the exact solution in figure 5.

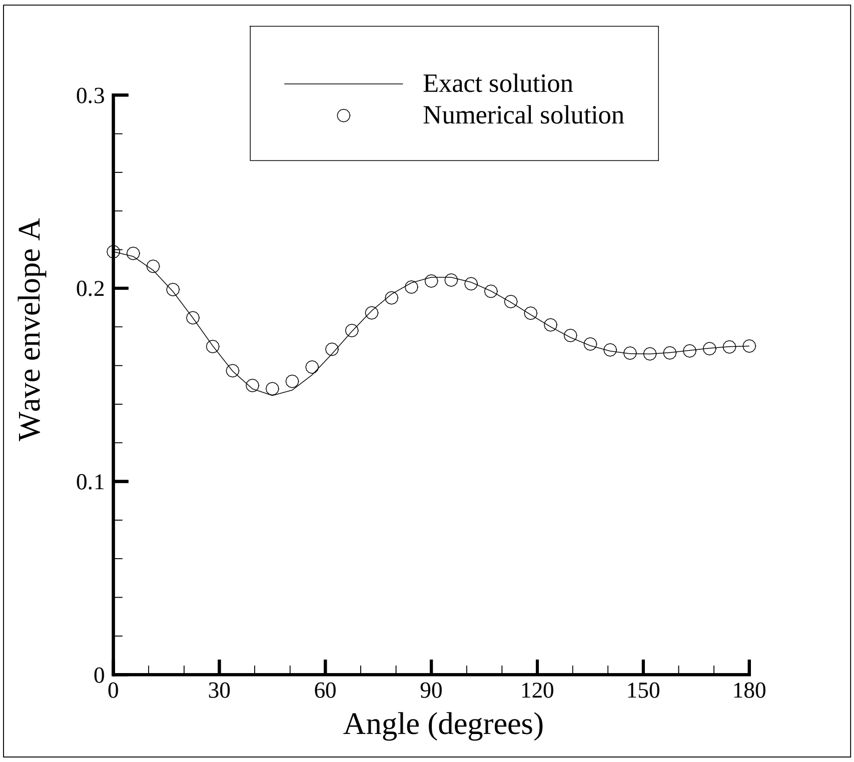

Figure 5: Variation in the amplitude along $r = 12$.

These values are obtained at the circumferential nodes situated at $r = 12$. As shown from figure 6 the relative error does not exceed 3.5 per cent

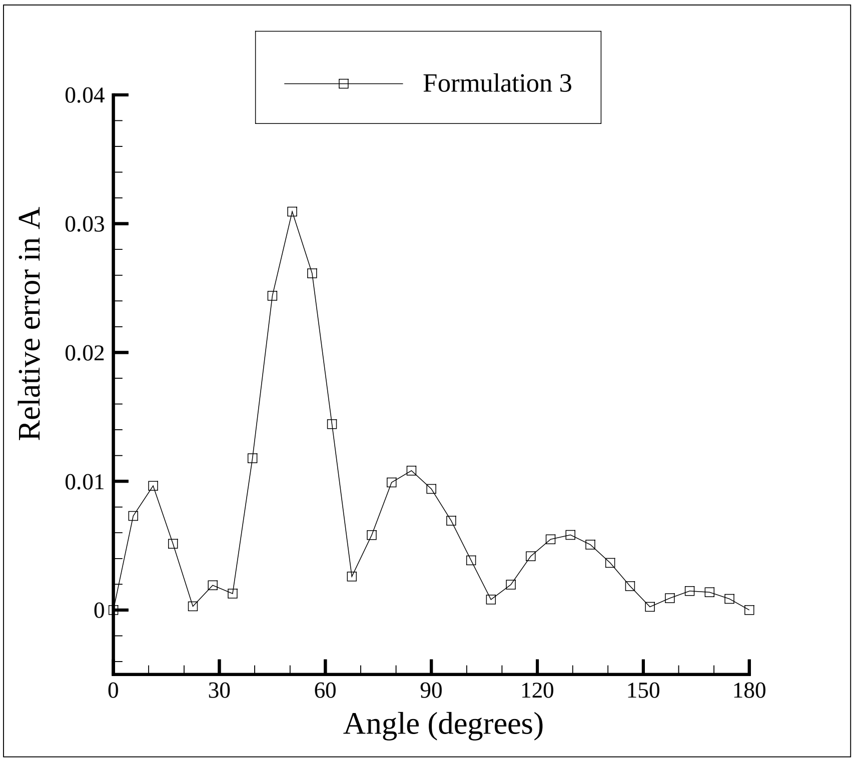

Figure 6: Relative error in wave envelope along $r = 12$.

which make the results acceptable. We now test the iteration procedure over domains containing finite and infinite elements.

6.2 Testing the iteration method

We test the iteration method by determining the potentials (31) and (32) in the region $r > 1$, $y > 0$ from the Dirichlet boundary condition on nodes on the arc $r = 1$ and on the boundary $y = 0$. We use an initial value for the phase in the iteration method by perturbing the exact value of the phase in this region by :

$$s_0 = s + \delta \sin(2\theta) \sin \frac{\pi}{2}(r - 1) \tag{33}$$

where s is the exact value for the phase, s_0 is the initial estimate and δ is a constant for each run. As the value of δ increases, the initial estimate for the phase becomes worse and we expect the number of iterations to increase. We test the iteration method by perturbing the phase of the two test potentials, starting with the diffraction potential. The iteration procedure is stopped when the imaginary part of the wave envelope is lower than 10^{-3}.

6.2.1 Modelling the Havelock diffraction potential

We consider the mesh given by figure 7 for the diffraction potential (32) with $\delta = 1$ and $k = \pi/2$. The finite region around the cylinder is meshed into 40 quadratic nine node finite elements and the infinite region is meshed into 8 ifinite elements.

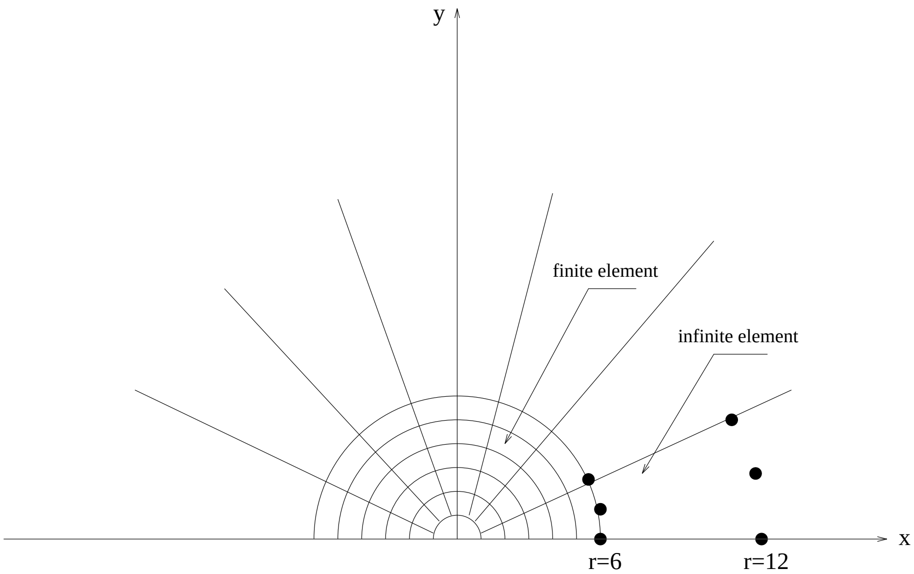

Figure 7: Mesh for Havelock diffraction potential.

We find that the method converges after 5 iterations. The iterated value for the wave envelope is given in figure 8.

In the following figure 9, we plot the wave envelope along $\theta = \pi/2$ for the initial solution, the first iteration, the fifth iteration and the exact solution. This shows how the wave envelope converges with successive iterations.

Also, for larger values of δ, the iteration method fails. We investigate further the relationship between the value of δ and the number of iterations needed for convergence next.

6.2.2 The robustness of the model

We test how robust the iteration method is for the Hankel source potential (32) over a mesh similar to the one given by figure 7.

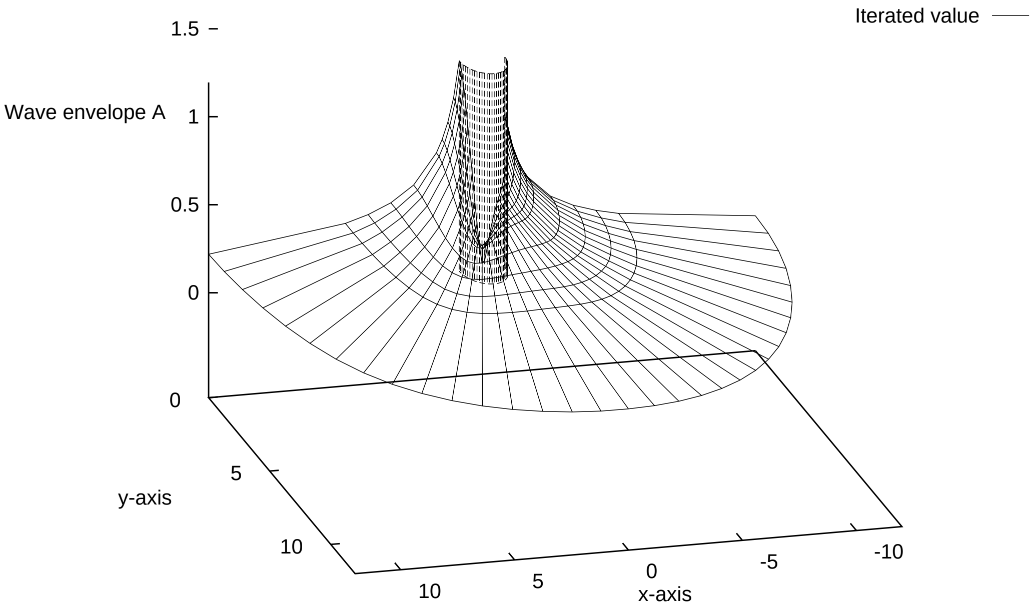

Figure 8: Iterated value of wave envelope, Havelock potential, $k = \pi/2$.

We consider the values for δ of 0.1 and 1, and in each case vary the wavenumber of the Hankel source potential. We can plot the number of iterations for each value of the wavenumber considered. The two plots are given below in figures 10 and 11.

We see that the two graphs are exponential, with a cut of wavenumber of 1.5π and 12π respectively beyond which the iteration method will not converge. However, we note that a value of $\delta = 1$ is a poor initial estimate for the phase gradient. It is probable that for a diffraction problem we can estimate the phase to of order less than $\delta = 0.1$. For an estimate of the phase to the order of $\delta = 0.1$, we can model the wave with a nodal spacing of around 2.5 wavelengths per nodal spacing, this refers to a value of the wavenumber of $k = 10\pi$. Since this is a 2-D problem, this is a mesh with around 500 times fewer nodal points than using a conventional potential mesh. If we can calculate the phase more accurately, then we can model for a higher value of the wavenumber. Finally, we present the results for the wave envelope variation with the wavenumber $k = 10\pi$.

The implications of the results are discussed in the next section.

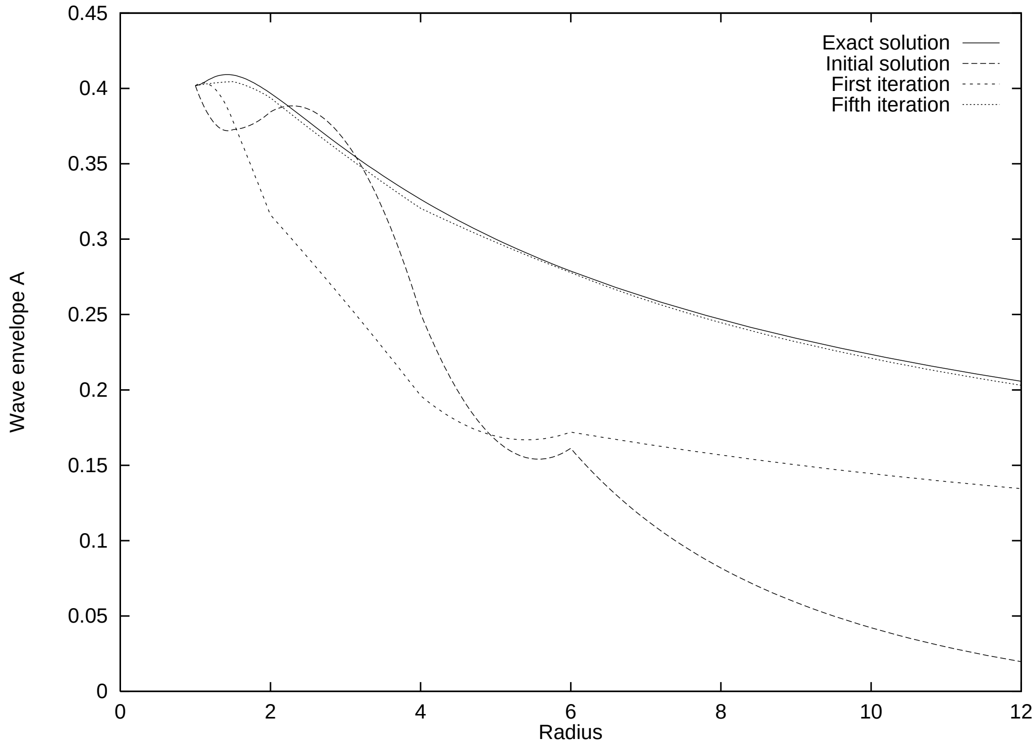

Figure 9: Variation in the amplitude along $\theta = \pi/2$.

7 Discussion

The present paper is an extension of the method for short wave diffraction problems proposed by Chadwick and Bettess [1] to incorporate infinite elements. This method iterates for the wave envelope and phase : An estimate for the phase is initially given from which the wave envelope and a better phase estimate is obtained. In the present paper, we introduce infinite elements and solve using the Dirichlet boundary condition. We first test different wave envelope infinite element formulations, choosing the one which is most accurate, then solve a diffraction potential problem, and finally investigate the convergence conditions for the phase estimate and wave number.

We present results for infinite elements where the phase is assumed to vary as the unit radius vector $\hat{r}$. The phase at nodal points within the element is therefore determined from the phase at nodal points on the finite/infinite element boundary. In obtaining the weak formulation of the governing integral, we generate an integration over a contour at infinity. We consider one formulation whereby this integral is evaluated, and another whereby Astley's

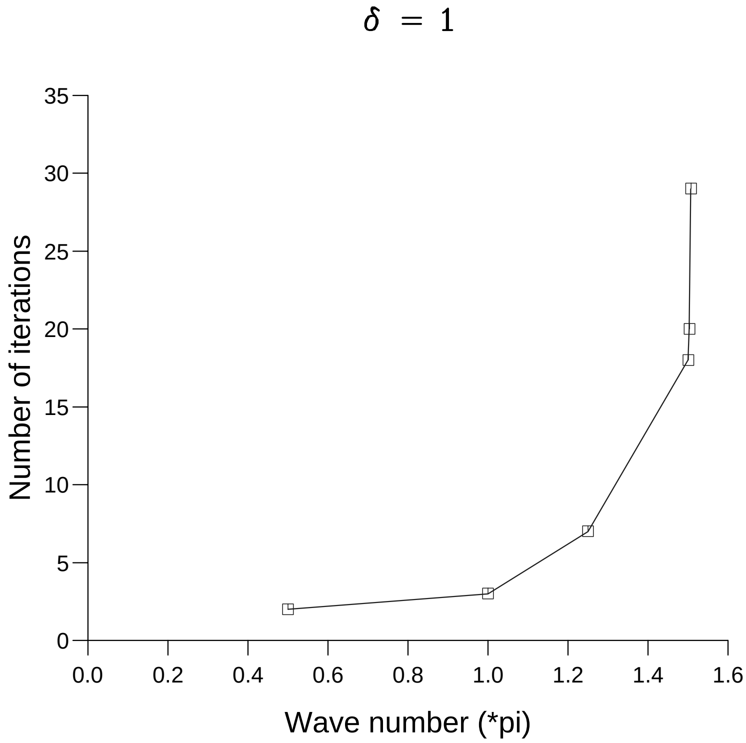

Figure 10: Number of iterations taken for convergence.

approach is used. In this the weighting functions are of lower order than the shape functions [7]. It is found that the Astley mapped wave envelope infinite element gives the best accuracy and so it is used for all subsequent results.

We then determine the Havelock diffraction potential for plane wave diffraction past a circular cylinder [14] given the value of the potential, the Dirichlet condition, on the boundary of the domain; Since the problem is symmetric, we consider one half of the domain only. The problem considered is for the cylinder radius a equal to unity, the wavenumber $k = \pi/2$, a mesh as given in figure 7. We perturb the phase and find that the method is successful and converges. However, the covergence depends upon the degree to which the phase is perturbed. For larger values of k for the diffraction potential, the wave envelope varies much more rapidly. In order to model the

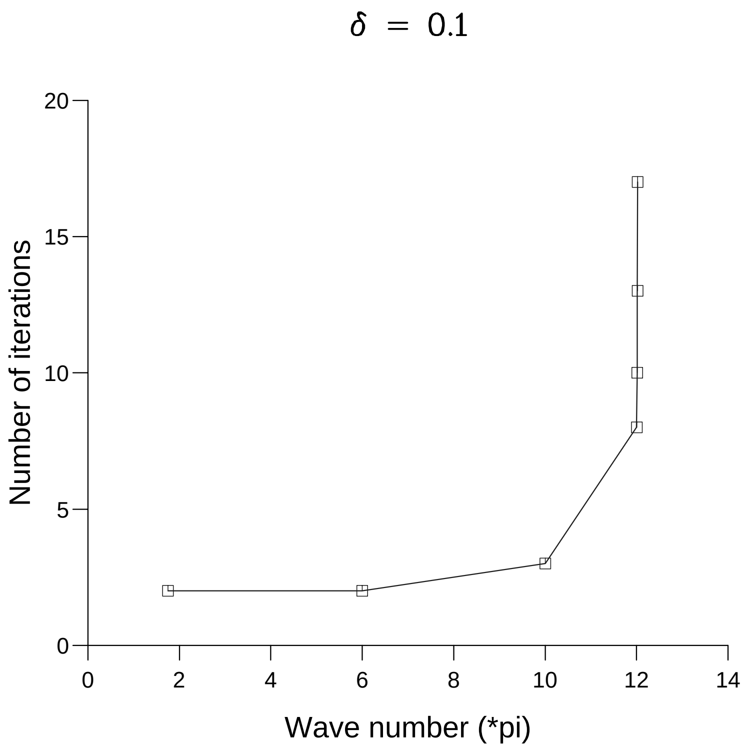

Figure 11: Number of iterations taken for convergence.

more rapid variation we should refine the mesh in the particular areas where this occurs. Automatic mesh adaptation, perhaps after each iteration, would therefore be of great use. However, this idea is not followed in the present paper.

Finally, we investigate the relation between the covergence, wavenumber, and estimate for the phase. This will give an idea how robust the model is. We use the Hankel source function (32) over the mesh given by figure 7. For a particular order of phase estimate, given by the value δ defined in (33), we plot the number of iterations taken to converge against the wavenumber. We find that these graphs have a cut off for a particular value of the wavenumber k beyond which the method will not converge. However, if a better estimate for the phase is initially chosen, then the cut of value for the wavenumber

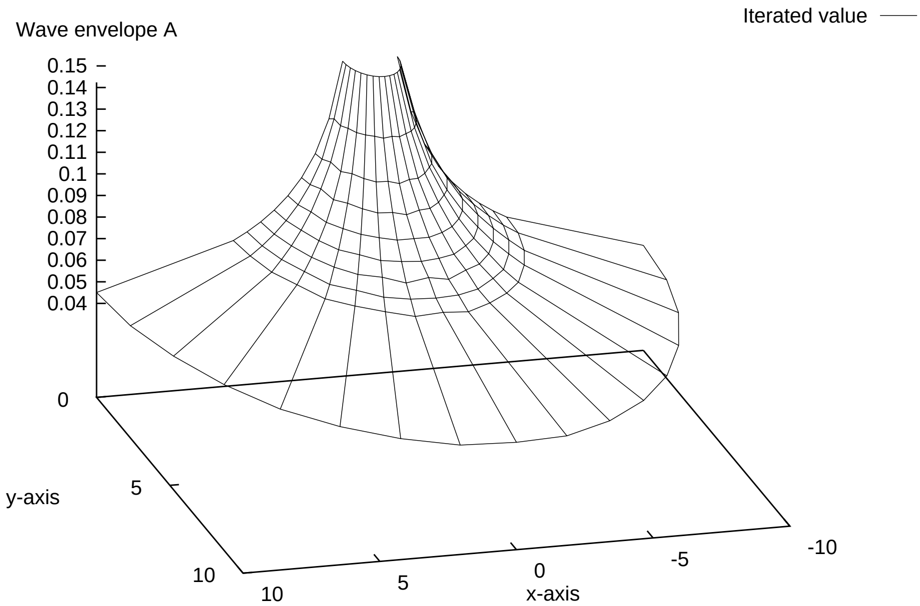

Figure 12: Iterated value of wave envelope : Hankel source, $k = 10\pi$.

k is greater. The results are impressive : for an initial error in the phase of order $\delta = 0.1$, we determine the Hankel source potential in the domain with around 500 times fewer nodal points than using a comparable conventional mesh. The iterated value of the wave envelope is plotted for this problem.

The method is therefore very promising. We believe evaluating the wave envelope and phase, rather than the potential, is the way forward for short wave diffraction problems. However, perhaps there is room for improvement on how the phase is evaluated. We note that the phase gradient gives a good approximation to the wave direction, and that the partition of unity finite element method developed by Melenk and Babuska [16] determines the wave direction implicitly at each node. We shall compare this methodology and the one presented in this paper for future work.

REFERENCES

1. E.A. Chadwick and P. Bettess, 'Modelling of progressive short waves using wave envelopes', *Int. Jour. Num. Meth. Eng.*, 1997. (accepted for publication)

2. O.C. Zienkiewicz and P. Bettess, 'Infinite elements in the study of fluid-structure interaction problems', *Computing methods in Applied Sciences, Lecture notes in Physics, Springer-Verlag, Berlin* **58**, 133-169, 1975.

3. P. Bettess and O.C. Zienkiewicz, 'Diffraction and refraction of surface waves using finite and infinite elements', *Int. Jour. Num. Meth. Eng.* **11**, 1271-1290, 1977.

4. O.C. Zienkiewicz, K. Bando, P. Bettess, C. Emson and T.C. Chiam, 'Mapped infinite elements for exterior wave problems', *Int. Jour. Num. Meth. Eng.* **21**, 1229-1251, 1985.

5. R.J.Astley, 'Wave envelope and infinite elements for acoustical radiation', *Int. Jour. Num. Meth. Fluids,* **3**, 507-526, 1983.

6. R.J. Astley and W. Eversman, 'Finite element formulation for acoustical radiation', *Jour. Sound and Vib.* **88(1)**, 47-64, 1983.

7. R.J. Astley, G.J. Macaulay and J.P. Coyette, 'Mapped wave envelope elements for acoustical radiation and scattering', *Jour. Sound and Vib.* **170(1)**, 97-118, 1994.

8. P. Bettess and E.A. Chadwick, 'Wave envelope examples for progressive waves', *Int. Jour. Num. Meth. Eng.* **38**, 2487-2508 (1995).

9. P. Bettess, *Infinite Elements*, Penshaw Press, Sunderland, U.K., 1992

10. H. Lamb, *Hydrodynamics*, Cambridge University Press, 1932

11. A. Sommerfeld, 'Theorie mathematique de la diffraction', *Math. Ann.*, **47**, 317-374, 1943.

12. F. Rellich, 'Uber das Asymptotische Verhalten der Losungen von $\Delta u + \lambda u = 0$ in Unendlichen Gebeiten', *Jahresbericht der Deutschen Mathematiker Voreinigung*, **53** 57-65, 1943.

13. A.M. Abramowitz and I.A. Stegun, *Handbook of Mathematical Functions*, New York, 1965

14. T.H. Havelock, 'The pressure of water waves upon a fixed obstacle', *Proc. Roy. Soc. Lon., Series A* No. 963 **175**, 409-421, 1940

15. R.C. MacCamy and R.A. Fuchs, 'Wave Forces on Piles. A Diffraction Theory', *Beach Erosion Board Tech. Mem. No. 69*, 1954.

16. J.M. Melenk and I. Babuska, 'The Partition of Unity Finite Element Method. Basic Theory and Applications', *Comput. Meths. Appl. Mech. Engrg.*, **139**, 289-314, 1996.

Appendix

We give the contour integral contributions at infinity explicitly in terms of the angles subtended by the element. Consider the contour integral given by

$$C_{kl} = \int_{-1}^{1} SF_j(\xi,\eta) SF_l(\xi,\eta) \frac{d\theta}{d\eta} d\eta \tag{34}$$

where

$$\begin{aligned}
SF_1 &= \frac{1}{2\sqrt{2}}\eta(1-\eta) \\
SF_2 &= -\eta(1-\eta) \\
SF_3 &= -\frac{1}{\sqrt{2}}(1-\eta)(1+\eta) \\
SF_4 &= 2(1-\eta)(1+\eta) \\
SF_5 &= -\frac{1}{2\sqrt{2}}\eta(1+\eta) \\
SF_6 &= \eta(1+\eta) \\
\frac{d\theta}{d\eta} &= \theta_1(-1/2+\eta) + \theta_2(-2\eta) + \theta_3(1/2+\eta)
\end{aligned}$$

Thus the integral contributions can be determined explicitly, and are given below from evaluations using maple:

$$\begin{aligned}
C_{11} &= .2000000000\theta_2 - .3333333333 * 10^{-1}\theta_3 - .1666666667\theta_1 \\
C_{12} &= -.56568542248\theta_2 + .9428090418 * 10^{-1}\theta_3 + .47140452206\theta_1 \\
C_{13} &= -.1000000000\theta_1 + .13333333333\theta_2 - .3333333333 * 10^{-1}\theta_3 \\
C_{14} &= .28284271124\theta_1 - .37712361165\theta_2 + .9428090416 * 10^{-1}\theta_3 \\
C_{15} &= .1666666667 * 10^{-1}\theta_1 - .1666666667 * 10^{-1}\theta_3 \\
C_{16} &= -.4714045208 * 10^{-1}\theta_1 + .4714045208 * 10^{-1}\theta_3 \\
C_{21} &= -.56568542248\theta_2 + .9428090418 * 10^{-1}\theta_3 + .47140452206\theta_1 \\
C_{22} &= 1.6000000000\theta_2 - .26666666667\theta_3 - 1.3333333333\theta_1 \\
C_{23} &= .28284271124\theta_1 - .37712361165\theta_2 + .9428090416 * 10^{-1}\theta_3 \\
C_{24} &= -.8000000000\theta_1 + 1.0666666667\theta_2 - .26666666667\theta_3 \\
C_{25} &= -.4714045208 * 10^{-1}\theta_1 + .4714045208 * 10^{-1}\theta_3 \\
C_{26} &= .13333333333\theta_1 - .13333333333\theta_3 \\
C_{31} &= -.1000000000\theta_1 + .13333333333\theta_2 - .3333333333 * 10^{-1}\theta_3 \\
C_{32} &= .28284271124\theta_1 - .37712361165\theta_2 + .9428090416 * 10^{-1}\theta_3
\end{aligned}$$

$$
\begin{aligned}
C_{33} &= -.2666666667\theta_1 + .2666666667\theta_3 \\
C_{34} &= .75424723331\theta_1 - .75424723331\theta_3 \\
C_{35} &= .3333333333 * 10^{-1}\theta_1 - .13333333333\theta_2 + .1000000000\theta_3 \\
C_{36} &= -.9428090416 * 10^{-1}\theta_1 + .37712361165\theta_2 - .28284271124\theta_3 \\
C_{41} &= .28284271124\theta_1 - .37712361165\theta_2 + .9428090416 * 10^{-1}\theta_3 \\
C_{42} &= -.8000000000\theta_1 + 1.066666667\theta_2 - .2666666667\theta_3 \\
C_{43} &= .75424723331\theta_1 - .75424723331\theta_3 \\
C_{44} &= -2.1333333333\theta_1 + 2.1333333333\theta_3 \\
C_{45} &= -.9428090416 * 10^{-1}\theta_1 + .37712361165\theta_2 - .28284271124\theta_3 \\
C_{46} &= .2666666667\theta_1 - 1.066666667\theta_2 + .8000000000\theta_3 \\
C_{51} &= .1666666667 * 10^{-1}\theta_1 - .1666666667 * 10^{-1}\theta_3 \\
C_{52} &= -.4714045208 * 10^{-1}\theta_1 + .4714045208 * 10^{-1}\theta_3 \\
C_{53} &= .3333333333 * 10^{-1}\theta_1 - .13333333333\theta_2 + .1000000000\theta_3 \\
C_{54} &= -.9428090416 * 10^{-1}\theta_1 + .37712361165\theta_2 - .28284271124\theta_3 \\
C_{55} &= .3333333333 * 10^{-1}\theta_1 - .2000000000\theta_2 + .1666666667\theta_3 \\
C_{56} &= -.9428090418 * 10^{-1}\theta_1 + .56568542248\theta_2 - .47140452206\theta_3 \\
C_{61} &= -.4714045208 * 10^{-1}\theta_1 + .4714045208 * 10^{-1}\theta_3 \\
C_{62} &= .13333333333\theta_1 - .13333333333\theta_3 \\
C_{63} &= -.9428090416 * 10^{-1}\theta_1 + .37712361165\theta_2 - .28284271124\theta_3 \\
C_{64} &= .2666666667\theta_1 - 1.066666667\theta_2 + .8000000000\theta_3 \\
C_{65} &= -.9428090418 * 10^{-1}\theta_1 + .56568542248\theta_2 - .47140452206\theta_3 \\
C_{66} &= .2666666667\theta_1 - 1.600000000\theta_2 + 1.3333333333\theta_3 \qquad (35)
\end{aligned}
$$